

# OPERATION OF LONGITUDINAL SHOCK WAVE FERROELECTRIC GENERATORS IN THE RESISTANCE MODE

S.I. Shkuratov<sup>1ξ</sup>, J. Baird<sup>1</sup>, E.F. Talantsev<sup>2</sup>, L.L. Altgilbers<sup>3</sup>

<sup>1</sup>*Loki Incorporated, Rolla, MO 65409, U.S.A.*

<sup>2</sup>*Pulsed Power LLC, Lubbock, TX 79416, U.S.A.*

<sup>3</sup>*U.S. Army Space and Missile Defense Command/Army Strategic Command, Huntsville, AL 35807, U.S.A.*

## Abstract

Results of systematic experimental investigations of operation of explosively driven longitudinal (shock wave propagates along the polarization vector **P**) shock wave ferroelectric generators (FEGs) with active loads varied in a wide range of resistance (more than 4 orders of magnitude) are presented. One of the specific features of FEGs is direct electrical connection of the ferroelectric energy-carrying element to the load. The ferroelectric element is always a part of the load circuit during explosive and electrical operation of the FEG. Electrical parameters of the ferroelectric element change significantly under shock wave action during operation of the generator and those changes affect the electrical parameters of the FEG-Load system. It follows from our experimental results that the output voltage, current and power produced by the FEG across the resistance load depend on both the electrical parameters of the load and geometrical dimensions of the ferroelectric energy-carrying element of the FEG. It is experimentally demonstrated that a miniature FEG is capable of delivering to the active load a pulsed power with peak amplitude up to 0.35 MW.

## I. INTRODUCTION

At ambient conditions, a solid solution of lead zirconate and lead titanate (PZT) in a Zr:Ti ratio of 95:5 with 2% doping with niobium [ $\text{Pb}_{0.99}(\text{Zr}_{0.95}\text{Ti}_{0.05})_{0.98}\text{Nb}_{0.02}\text{O}_3$ , denoted by PZT 95/5-2Nb or PZT 95/5] is a ferroelectric (FE) phase with a rhombohedral structure, but it is near the boundary of an antiferroelectric (AFE) phase having an orthorhombic structure [1]. At a hydrostatic pressure of approximately 0.4 GPa, the FE-to-AFE polymorphic phase transition occurs [1].

If the PZT 95/5 ferroelectric sample was previously poled, the FE-to-AFE phase transition results in a sudden release of a bounded electric charge at the contact plates of the sample. This effect can be used for generation of primary electrical power. The first attempts to utilize the FE-to-AFE phase transition through the shock compressi-

on of PZT 95/5 ferroelectrics to generate primary pulsed power were started more than 40 years ago [2] and they continue [3].

Successful shock initiated FE-to-AFE phase transition in the PZT 95/5 is based on an assumption that the ceramic is free from porous and other 3D defects. This is not the case, however, for real ceramic samples [4]. Understanding and theoretical description of the depolarization process in shock-compressed PZT 95/5 ceramic samples is very uncertain due to the fact that the samples are not just shock-compressed, but also shock-heated and subjected to other shock-related effects [5]. In addition, shock-induced phase-structural transformations occur in the sample along with the depolarization process.

Our approach to the generation of primary pulsed power with ferroelectric materials [6,7] is different from that described above. It is based on the idea that shock compression of the poled ferroelectric samples is strong enough to provide the release of bonded charges without an initiation of FE-to-AFE phase transition. In our opinion it is almost not possible that anti-ferroelectric phase state (that is a specific kind of magnetic ordering of the ferroelectric state) can be created with a totally destructive shock-wave impact associated with highly intense shock heat and ultimate shock pressure. Our approach is based on the assumption that phase transformation in shocked ferroelectrics would be more like FE-to-non-FE. It means that ferroelectric materials having chemical compositions far from phase transition boundaries are capable to release its polarization charge under the shock wave action. If the PZT 95/5 is closed to FE-to-AFE phase boundary [8], the ferroceramics  $\text{Pb}(\text{Zr}_{0.52}\text{Ti}_{0.48})\text{O}_3$  (denoted by PZT 52/48) is exactly on the morphotronic phase boundary (MPB) (i.e. between the tetragonal ferroelectric phase and the rhombohedral ferroelectric phase). It should be noted that all PZT compounds near the MPB have maximum coupling coefficient and maximum relative permittivity which are important for engineering applications of ferroceramics [8].

The mechanism of the release of the electric charge in shocked ferroelectric samples would include several physical and structural processes. For instance, this mechanism could definitely utilize ceramic porosity. It was recently demonstrated [9] that spherical micron size

<sup>ξ</sup> E-mail: shkuratov@lokiconsult.com

Report Documentation Page				Form Approved OMB No. 0704-0188	
Public reporting burden for the collection of information is estimated to average 1 hour per response, including the time for reviewing instructions, searching existing data sources, gathering and maintaining the data needed, and completing and reviewing the collection of information. Send comments regarding this burden estimate or any other aspect of this collection of information, including suggestions for reducing this burden, to Washington Headquarters Services, Directorate for Information Operations and Reports, 1215 Jefferson Davis Highway, Suite 1204, Arlington VA 22202-4302. Respondents should be aware that notwithstanding any other provision of law, no person shall be subject to a penalty for failing to comply with a collection of information if it does not display a currently valid OMB control number.					
1. REPORT DATE <b>JUN 2009</b>		2. REPORT TYPE <b>N/A</b>		3. DATES COVERED <b>-</b>	
4. TITLE AND SUBTITLE <b>Operation Of Longitudinal Shock Wave Ferroelectric Generators In The Resistance Mode</b>				5a. CONTRACT NUMBER	
				5b. GRANT NUMBER	
				5c. PROGRAM ELEMENT NUMBER	
6. AUTHOR(S)				5d. PROJECT NUMBER	
				5e. TASK NUMBER	
				5f. WORK UNIT NUMBER	
7. PERFORMING ORGANIZATION NAME(S) AND ADDRESS(ES) <b>U.S. Army Space and Missile Defense Command/Army Strategic Command, Huntsville, AL 35807, U.S.A.</b>				8. PERFORMING ORGANIZATION REPORT NUMBER	
9. SPONSORING/MONITORING AGENCY NAME(S) AND ADDRESS(ES)				10. SPONSOR/MONITOR'S ACRONYM(S)	
				11. SPONSOR/MONITOR'S REPORT NUMBER(S)	
12. DISTRIBUTION/AVAILABILITY STATEMENT <b>Approved for public release, distribution unlimited</b>					
13. SUPPLEMENTARY NOTES <b>See also ADM002371. 2013 IEEE Pulsed Power Conference, Digest of Technical Papers 1976-2013, and Abstracts of the 2013 IEEE International Conference on Plasma Science. IEEE International Pulsed Power Conference (19th). Held in San Francisco, CA on 16-21 June 2013.</b>					
14. ABSTRACT <b>Results of systematic experimental investigations of operation of explosively driven longitudinal (shock wave propagates along the polarization vector P) shock wave ferroelectric generators (FEGs) with active loads varied in a wide range of resistance (more than 4 orders of magnitude) are presented. One of the specific features of FEGs is direct electrical connection of the ferroelectric energy-carrying element to the load. The ferroelectric element is always a part of the load circuit during explosive and electrical operation of the FEG. Electrical parameters of the ferroelectric element change significantly under shock wave action during operation of the generator and those changes affect the electrical parameters of the FEG-Load system. It follows from our experimental results that the output voltage, current and power produced by the FEG across the resistance load depend on both the electrical parameters of the load and geometrical dimensions of the ferroelectric energy-carrying element of the FEG. It is experimentally demonstrated that a miniature FEG is capable of delivering to the active load a pulsed power with peak amplitude up to 0.35 MW.</b>					
15. SUBJECT TERMS					
16. SECURITY CLASSIFICATION OF:			17. LIMITATION OF ABSTRACT <b>SAR</b>	18. NUMBER OF PAGES <b>6</b>	19a. NAME OF RESPONSIBLE PERSON
a. REPORT <b>unclassified</b>	b. ABSTRACT <b>unclassified</b>	c. THIS PAGE <b>unclassified</b>			



pores in energetic materials are transformed into enormous growing fractal-type cracks behind the shock wave front. Similar effects may take place in the shocked ferroelectric ceramic samples. Thus, bounded charges could be quickly released in the compressed part of the ferroceramics.

Since the end of 1990s, we have been performing systematic studies of pulsed power generation with compact explosive driven ferroelectric generators utilizing longitudinal shock compression of poled PZT 52/48 ceramic samples.

In our previous work [10,11], we performed systematic experimental and modeling studies of pulsed power generation with the ferroelectric generators based on longitudinally shocked (shock wave propagated along the depolarization vector  $\mathbf{P}$ ) PZT 52/48 ceramic samples loaded with practical loads, capacitor banks that were a prototypes of the miniature Marx generator capacitors bank.

In this work, we extended this research line and performed experimental studies of pulsed power generation with longitudinal shock wave ferroelectric generators (FEGs) loaded with ohmic loads over a wide range of load resistance (about 5 orders of magnitude).

## II. RESULTS AND DISCUSSION

A schematic diagram of the experimental setup for studies of the operation of the longitudinal shock wave FEG in the resistance mode is shown in Fig. 1. It contains an explosively driven longitudinal FEG, a load circuit and a pulse measuring system.

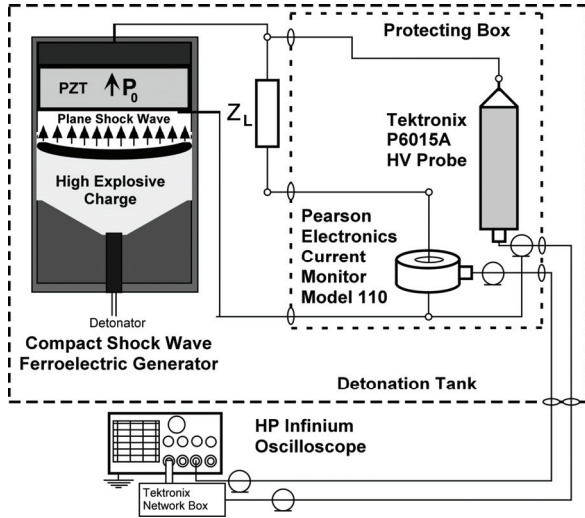
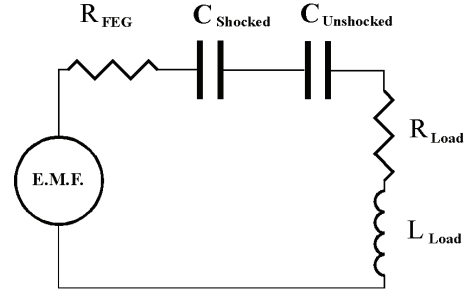


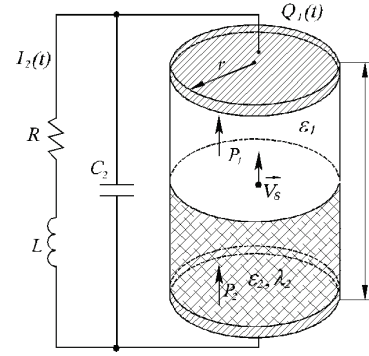
**Figure 1.** Schematic diagram of the experimental setup for investigating the operation of the explosive-driven FEG in the resistance mode.

The load of the FEG was made of low-inductance 2-watt bulk carbon composition resistors. For each load, from three to five resistors were connected in series to

avoid electrical breakdown along their surfaces. The inductance of the load units did not exceed 230 nH.



(a)



(b)

**Figure 2.** Equivalent circuit of the FEG operating in the resistance mode.

Pearson Electronics current monitors, models 411 and 110, were used for measurement of the pulsed current. A Tektronix P6015A high-voltage probe was used to monitor the FEG output voltage. Pulsed signals were recorded with an HP Agilent 54845A oscilloscope (bandwidth 1.5 GHz, 8 GSa/s) and a Tektronix TDS2024 oscilloscope (bandwidth 200 MHz, 2 GSa/s). The explosive driven FEGs were placed in a detonation chamber. The load, measuring circuits and pulse recording equipment were placed outside the detonation chamber. Other experimental details are described in [6, 10-13].

The equivalent circuit of the FEG operating in the resistance mode is shown in Fig. 2. The FEG-Load system is represented as an RC-circuit, but it is not a conventional RC-circuit. The ferroelectric energy-carrying element of the FEG is a dynamic capacitor that is charged due to shock wave depolarization of the ferromodule, and it is immediately discharged through the load. The capacitance of the shock-compressed part of the ferroelectric element is represented in the circuit as  $C_{Shocked}$  [Fig. 2(a)], and the capacitance of uncompressed part of element is as  $C_{Unshocked}$ . Shock wave compression changes the electrical and physical properties of ferroelectric materials significantly. The permittivity (and the capacitance) of

shock-compressed ferroelectric materials is a function of the parameters of the shock wave. The electrical conductivity of shock-compressed part of the ferroelectric element can be higher than that of uncompressed part. The parameter  $R_{FEG}$  represents the resistance of the shock-compressed part of the ferroelectric element in the equivalent circuit of the FEG-Load system [Fig. 2(a)].  $R_{Load}$  and  $L_{Load}$  are resistance and inductance of the load, respectively. The E.M.F. represents the electric charge released at the contact plates of the ferroelectric element due to its shock wave depolarization.

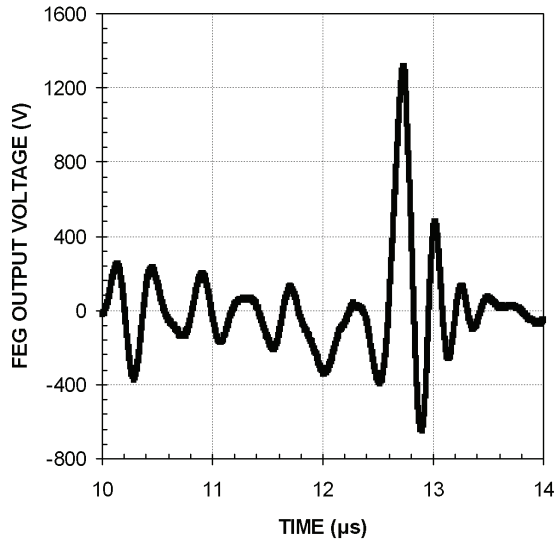


**Figure 3.** A typical waveform of the high-voltage pulse produced by the FEG containing a PZT 52/48 element of  $D = 26.0 \text{ mm/h} = 0.65 \text{ mm}$  across  $0.7\text{-}\Omega$  load.

#### A. Low resistance loads

To get information about operation of FEGs with low resistance loads we performed a series of experiments with FEGs containing thin PZT 52/48 element of  $26.0 \text{ mm}$  diameter ( $D$ ) and  $0.65 \text{ mm}$  thickness ( $h$ ). A typical waveform of the voltage pulse produced by an FEG containing a PZT 52/48 element of  $D = 26.0 \text{ mm/h} = 0.65 \text{ mm}$  across a  $0.7\text{-}\Omega$  load is shown in Fig. 3. The voltage oscillated with an obvious maximum in the voltage waveform. The peak amplitude of the voltage pulse was  $U(12.7 \text{ }\mu\text{s})_{\text{max}} = 1.31 \text{ kV}$  with full width at half the maximum (FWHM) of  $0.1 \text{ }\mu\text{s}$ , and risetime  $\tau = 0.1 \text{ }\mu\text{s}$ .

Corresponding waveforms of the output current  $I(t)$ , voltage  $U(t)$ , and power  $P(t)$  pulses produced by an FEG across a  $0.7\text{-}\Omega$  load are shown in Fig. 4. The peak output current was  $I(t = 12.6 \text{ }\mu\text{s})_{\text{max}} = 308.0 \text{ A}$ .

The power dissipated by the load was calculated as the product of the instantaneous value of the output voltage  $U(t)$  and the instantaneous current in the circuit,  $I(t)$ :  $P(t) = I(t) \cdot U(t)$ . So, the peak power delivered from the FEG to a  $0.7\text{-}\Omega$  load was  $P(12.7 \text{ }\mu\text{s})_{\text{max}} = 301 \text{ kW}$ . This was more

than seven times higher than the power delivered to the same load by an FEG containing a PZT 52/48 element of  $D = 25.0 \text{ mm/h} = 2.5 \text{ mm}$ . A thin PZT 52/48 element possessing higher initial capacitance provided significantly higher power to the low-resistance load. The average peak power delivered to the load in this series of experiments was  $P_{\text{aver}} = 328 \pm 24 \text{ kW}$ .

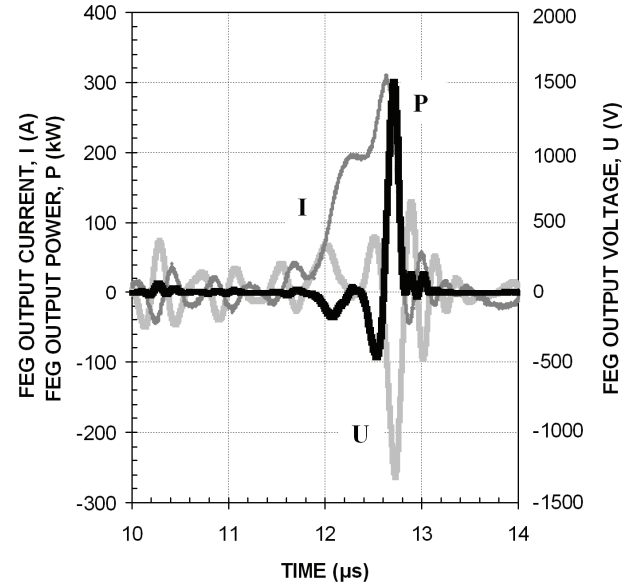


**Figure 4.** Corresponding (Fig. 3) waveforms of the output current,  $I(t)$ , (dark gray), voltage,  $U(t)$ , (light gray) and power,  $P(t)$ , (black) pulses produced by the FEG containing a PZT 52/48 element of  $D = 26.0 \text{ mm/h} = 0.65 \text{ mm}$  across a  $0.7\text{-}\Omega$  load.

Integration of the  $P(t)$  waveform from 0 to  $t$  gives the momentary value of the energy,  $W(t)$ , delivered to the resistance load during explosive operation of the FEG:

$$W(t) = \int_0^t P(t) \cdot dt \quad (1)$$

The energy delivered from the FEG to the  $0.7\text{-}\Omega$  load was  $41 \text{ mJ}$ . Average energy delivered to the load in this series of experiments was  $W_{\text{aver}} = 42 \pm 5 \text{ mJ}$ .

#### B. Medium resistance loads

A typical waveform of the high-voltage pulse produced by an FEG containing a PZT 52/48 element of  $D = 25.0 \text{ mm/h} = 2.5 \text{ mm}$  across a  $40\text{-}\Omega$  load is shown in Fig. 5. The amplitude of the voltage pulse produced by an FEG across the load was  $U(13.2 \text{ }\mu\text{s})_{\text{max}} = 3.63 \text{ kV}$ . The FWHM of the pulse was  $1.1 \text{ }\mu\text{s}$  and risetime  $\tau = 1.0 \text{ }\mu\text{s}$ . The maximum electric field strength reached in the ferroelectric element in this experiment was  $1.73 \text{ kV/mm}$ . The high-voltage pulse amplitude averaged from the three experiments of this series was  $U(t)_{\text{aver}} = 3.6 \pm 0.07 \text{ kV}$ .

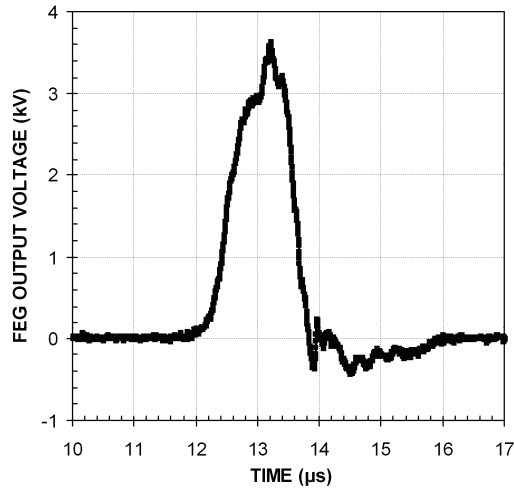


**Figure 5.** A typical waveform of the high-voltage pulse produced by the FEG containing a PZT 52/48 element of  $D = 25.0 \text{ mm/h} = 2.5 \text{ mm}$  across  $40\text{-}\Omega$  load.

The waveforms of the output current  $I(t)$ , high voltage  $U(t)$ , and power  $P(t)$  pulses produced by an FEG across  $40\text{-}\Omega$  load are shown in Fig. 6. The peak output current was  $I(13.3 \text{ }\mu\text{s})_{\text{max}} = 85.4 \text{ A}$ . The peak power delivered to the  $40\text{-}\Omega$  load was  $P(13.3 \text{ }\mu\text{s})_{\text{max}} = 321 \text{ kW}$ , and the average peak power delivered to the load in this series of experiments was  $P_{\text{aver}} = 314 \pm 11 \text{ kW}$ .

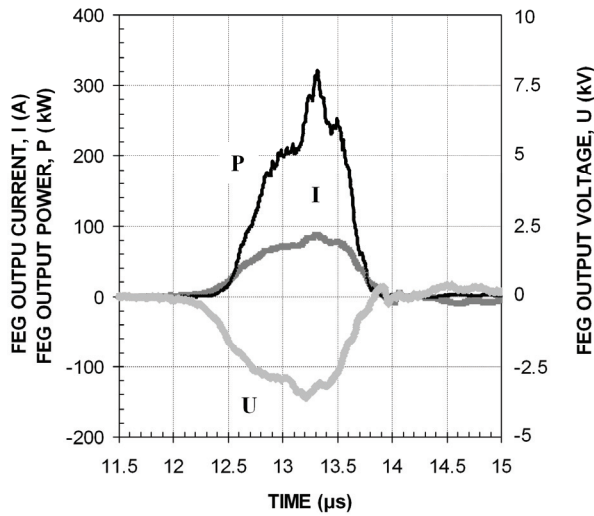


**Figure 6.** Waveforms of the output current,  $I(t)$ , (dark gray), voltage,  $U(t)$ , (light gray) and power,  $P(t)$ , (black) pulses produced by the FEG containing a PZT 52/48 element of  $D = 25.0 \text{ mm/h} = 2.5 \text{ mm}$  across  $40\text{-}\Omega$  load.

The maximum energy delivered to the  $40\text{-}\Omega$  load in this experiment was  $W_{\text{max}} = 225 \text{ mJ}$ . The average energy delivered to the load in experiments of this series was  $W_{\text{aver}} = 219 \pm 18 \text{ mJ}$ . The specific energy density of the PZT 52/48 element in these experiments was  $W_{\text{spec aver}} = 182.5 \pm 15.0 \text{ mJ/cm}^3$ .

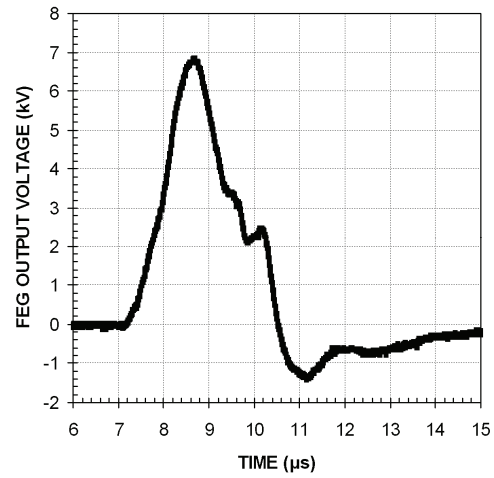


**Figure 7.** A typical waveform of the high-voltage pulse produced by an FEG containing a PZT 52/48 element of  $D = 25.0 \text{ mm/h} = 5.1 \text{ mm}$  across a  $300\text{-}\Omega$  load.

### C. High resistance loads

Figures 7 and 8 presents a typical waveform of a high-voltage pulse produced by an FEG containing a PZT 52/48 element of  $D = 25.0 \text{ mm/h} = 5.1 \text{ mm}$  across a  $300\text{-}\Omega$  load, and the corresponding waveforms of output current and power. The amplitude of the voltage pulse was  $U(8.7 \text{ }\mu\text{s})_{\text{max}} = 6.82 \text{ kV}$ , FWHM was  $1.52 \text{ }\mu\text{s}$  and risetime  $\tau = 1.5 \text{ }\mu\text{s}$ . The maximum electric field strength reached in the ferroelectric element in this experiment was  $1.34 \text{ kV/mm}$ . The high-voltage pulse amplitude averaged from three experiments of this series was  $U(t)_{\text{aver}} = 6.77 \pm 0.71 \text{ kV}$ .

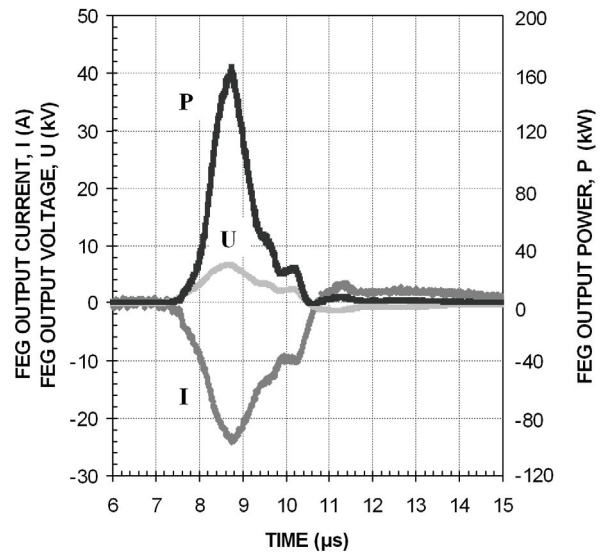


**Figure 8.** Typical waveforms (corresponding to Fig. 7) of the output current  $I(t)$  (dark gray), voltage  $U(t)$  (light gray), and power  $P(t)$  (black) produced by the FEG containing a PZT 52/48 element of  $D = 25.0 \text{ mm/h} = 5.1 \text{ mm}$  across a  $300\text{-}\Omega$  load.

The maximum energy delivered to the 300- $\Omega$  load in this experiment was  $W_{\max} = 186$  mJ. The energy averaged over the three experiments of this series was  $W_{\text{aver}} = 181.4 \pm 12.7$  mJ. The specific energy density of the PZT 52/48 element in these experiments was  $W_{\text{spec aver}} = 72.4 \pm 5.1$  mJ/cm<sup>3</sup>.

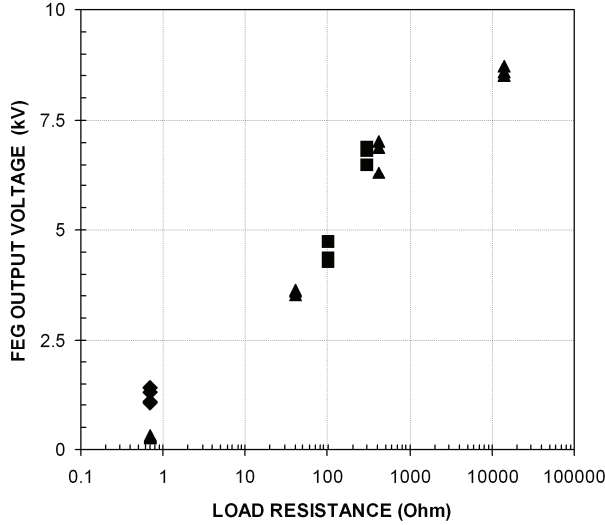


**Figure 9.** The amplitude of voltage pulse produced by FEGs containing PZT 52/48 elements of  $D = 26.0$  mm/h = 0.65 mm (diamonds),  $D = 25.0$  mm/h = 2.5 mm (triangles) and  $D = 25.0$  mm/h = 5.1 mm (squares) versus resistance of the load.

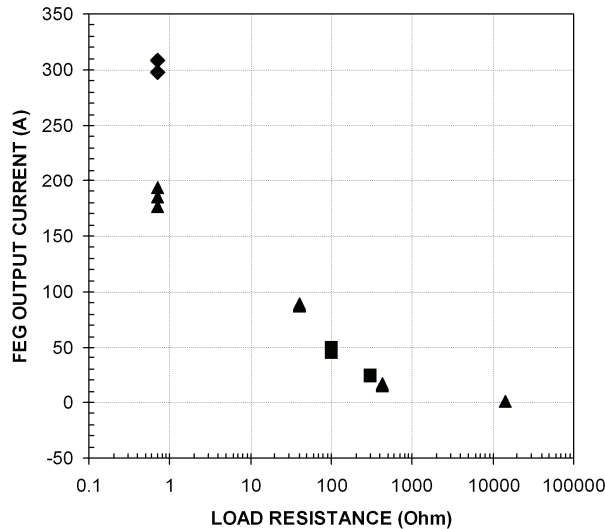


**Figure 10.** The amplitude of current pulse in the active load circuit versus resistance of the load produced by FEGs containing PZT 52/48 elements of  $D = 26.0$  mm/h = 0.65 mm (diamonds),  $D = 25.0$  mm/h = 2.5 mm (triangles) and  $D = 25.0$  mm/h = 5.1 mm (squares).

#### D. Experimental result summary

In addition to the experiments described above, extensive studies were also performed for FEGs with a 14-k $\Omega$  resistance load. Thus, in the series of experiments described in this paper, the resistance of the load was varied in the range from 0.7  $\Omega$  to 14 k $\Omega$ . Results of experiments with FEGs containing PZT 52/48 elements of  $D = 26.0$  mm/h = 0.65 mm,  $D = 25.0$  mm/h = 2.5 mm and  $D = 25.0$  mm/h = 5.1 mm re shown in Figs. 9 through 11.

Figure 9 presents the amplitudes of voltage pulses produced by FEGs versus resistance of the load. Because of the wide range of load resistances, the X-axis (Load Resistance) of the graph is a logarithmic scale. Our experimental results show that increasing the load resistance leads to an increase of the voltage produced by the FEG.

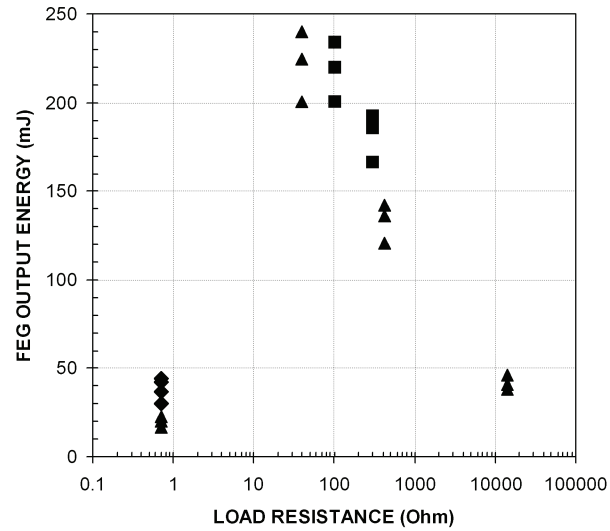


**Figure 11.** Energy delivered to the load from FEGs containing PZT 52/48 elements of  $D = 26.0$  mm/h = 0.65 mm (diamonds),  $D = 25.0$  mm/h = 2.5 mm (triangles) and  $D = 25.0$  mm/h = 5.1 mm (squares).

The voltage vs. resistance plot is practically linear in a logarithmic scale for the resistance axis (Fig. 9). This result is new and has never been reported by others, and it is very important in the understanding of shock compressed ferroelectric physics.

Figure 10 summarizes the amplitudes of current generated by FEGs in a load circuit. The current amplitude is inversely proportional to the load resistance. The maximum current of 308 A was reached with a load of resistance 0.7  $\Omega$ . In this resistance range, the FEG output current has inverse exponential dependence on the load resistance.

Figure 11 summarizes results of experiments concerning the energy delivered from the FEGs in the loads. It follows from our experimental results (Figs. 11) that there is an optimum load resistance at which the FEG provides the maximum output power and energy.



### III. SUMMARY

Systematic experimental investigations of the operation of explosively driven longitudinal shock wave FEGs with active loads in a wide range (more than 4 orders of magnitude) of resistance were performed. The experimental results show that the output voltage, current, and power produced by the FEG across the resistance load depend on both the electrical parameters of the load and on the geometrical dimensions of the ferroelectric energy-carrying element of the FEG. We experimentally demonstrated that a miniature FEG is capable of delivering pulsed power with a peak amplitude up to 0.35 MW to an active load.

New fundamental experimental results revealing the logarithmic dependence of the voltage generated by the FEG containing PZT 52/48 ferroceramics across the active load, versus the resistance of the load, were obtained in this work.

### IV. REFERENCES

- [1] I.J. Fritz, "Uniaxial-stress effects in a 95/5 lead zirconate titanate ceramic," *J. Appl. Phys.*, vol. 49, pp. 4922-4928, 1978.
- [2] W.J. Halpin, "Current from a shock-loaded short-circuited ferroelectric ceramic disk", *J. Appl. Phys.*, vol. 37, pp. 153-163, 1966.
- [3] R.E. Setchell, "Shock wave compression of the ferroelectric ceramic  $\text{Pb}_{0.99}(\text{Zr}_{0.95}\text{Ti}_{0.05})_{0.98}\text{Nb}_{0.02}\text{O}_3$ : depoling currents," *J. Appl. Phys.*, vol. 97, No. 015307, 2005.
- [4] R.E. Setchell, "Shock wave compression of the ferroelectric ceramic  $\text{Pb}_{0.99}(\text{Zr}_{0.95}\text{Ti}_{0.05})_{0.98}\text{Nb}_{0.02}\text{O}_3$ : microstructural effects," *J. Appl. Phys.*, vol. 101, No. 053525, 2007.
- [5] E.J. Reed, M.R. Armstrong, K. Kim, M. Soljagic, J.H. Glowina, J.D. Joannopoulos, "Terahertz radiation from shocked materials," *Materials Today*, Vol. 10, Issue 7-8, pp.44-50, 2007.
- [6] S.I. Shkuratov, E.F. Talantsev, L. Menon, H. Temkin, J. Baird, and L.L. Altgilbers, "Compact high-voltage generator of primary power based on shock wave depolarization of lead zirconate titanate piezoelectric ceramics," *Review of Scientific Instruments*, vol. 75, pp. 2766-2769, 2004.
- [7] S.I. Shkuratov, E.F. Talantsev, J. Baird, H. Temkin, L.L. Altgilbers, A.H. Stults, "Longitudinal shock wave depolarization of  $\text{Pb}(\text{Zr}_{52}\text{Ti}_{48})\text{O}_3$  polycrystalline ferroelectrics and their utilization in explosive pulsed power," *AIP Conference Proceedings*, vol. 845, Part II, pp. 1169-1172, 2006.
- [8] M.J. Haun, E. Furman, S.J. Jang, and L.E. Cross, "Thermodynamic theory of the lead zirconate-titanate solid solution system, part I: phenomenology," *Ferroelectrics*, vol. 99, pp. 13-25, 1989.
- [9] N.R. Barton, N.W. Winter and J.E. Reaugh, "Defect evolution and pore collapse in crystalline energetic materials," *Modelling Simul. Mater. Sci. Eng.*, vol. 17, Article number 035003, 2009.
- [10] S.I. Shkuratov, E.F. Talantsev, J. Baird, Y. Tkach, L.L. Altgilbers, A.H. Stults, S.V. Kolossenok, "Pulsed charging of capacitor bank by compact explosive-driven high-voltage primary power source based on longitudinal shock wave depolarization of ferroelectric ceramics," *Digest of Technical Papers - IEEE International Pulsed Power Conference*, Article number 4084270, pp. 537-540, 2007.
- [11] S.I. Shkuratov, J. Baird, E.F. Talantsev, A.V. Ponomarev, L.L. Altgilbers, A.H. Stults, "High voltage charging of a capacitor bank," *IEEE Trans. Plasma Science*, vol. 36, pp. 44-51, 2008.
- [12] Y. Tkach, S.I. Shkuratov, E.F. Talantsev, J.C. Dickens, M. Kristiansen, L.L. Altgilbers, P.T. Tracy, "Theoretical treatment of explosive-driven ferroelectric generators," *IEEE Trans. Plasma Science*, vol. 30, Issue 5, Part I, pp. 1665-1673, 2002.
- [13] S.I. Shkuratov, E.F. Talantsev, J. Baird, H. Temkin, Y. Tkach, L.L. Altgilbers, A.H. Stults, "Depolarization of a  $\text{Pb}(\text{Zr}_{52}\text{Ti}_{48})\text{O}_3$  polycrystalline piezoelectric energy-carrying element of compact pulsed power generator by a longitudinal shock wave," *Digest of Technical Papers - IEEE International Pulsed Power Conference*, Article number 4084268, pp. 529-532, 2007.